

## Accelerated disintegration of compostable Ecovio polymer by using ZnO particles as filler



Adolfo del Campo<sup>a</sup>, Eva de Lucas-Gil<sup>a</sup>, Fernando Rubio-Marcos<sup>a,f</sup>, Marina P. Arrieta<sup>b,c</sup>, Marta Fernández-García<sup>d,e</sup>, José F. Fernández<sup>a</sup>, Alexandra Muñoz-Bonilla<sup>d,e,\*</sup>

<sup>a</sup> Electroceramic Department, Instituto de Cerámica y Vidrio, CSIC, Kelsen 5, 28049 Madrid, Spain

<sup>b</sup> Departamento de Ingeniería Química Industrial y del Medio Ambiente, Escuela Politécnica Superior de Ingenieros Industriales, Universidad Politécnica de Madrid (ETSII-UPM), C/José Gutiérrez Abascal 2, 28006 Madrid, Spain

<sup>c</sup> Grupo de Investigación: Polímeros, Caracterización y Aplicaciones (POLCA), 28006 Madrid, Spain

<sup>d</sup> Instituto de Ciencia y Tecnología de Polímeros (ICTP-CSIC), C/Juan de la Cierva 3, 28006 Madrid, Spain

<sup>e</sup> Interdisciplinary Platform for Sustainable Plastics towards a Circular Economy-Spanish National Research Council (SusPlast-CSIC), 28006 Madrid, Spain

<sup>f</sup> Escuela Politécnica Superior, Universidad Antonio de Nebrija, Pirineos 55, 28040, Madrid, Spain

### ARTICLE INFO

#### Article history:

Received 16 November 2020

Revised 20 January 2021

Accepted 24 January 2021

Available online 28 January 2021

### ABSTRACT

ZnO compounds exert a catalytic effect on the degradation of polyesters and could affect the biodegradability of such polymers. Herein, composites of 2 wt% of ZnO particles and biodegradable commercial Ecovio polymer, a blend of poly(lactic acid) (PLA) and a copolyester, are prepared by melt extrusion process to further study the effect of the incorporation of ZnO particles on the biodegradability of this polyester under composting conditions. Different nano- and micro-sized ZnO particles are employed to investigate the effect of the size, morphology, and surface charge of ZnO on the physicochemical properties of the polymeric composite and nanocomposite by differential scanning calorimetry (DSC) and thermogravimetric analyses (TGA). The influence of such compounds on the compost disintegrability is further investigated by different techniques including, gel permeation chromatography (GPC), confocal Raman microscopy and energy dispersive x-ray spectrometer (EDX). The results demonstrate that the ZnO particles significantly accelerate the disintegration process of the Ecovio polymeric blend under a composting environment.

© 2021 Elsevier Ltd. All rights reserved.

### 1. Introduction

Biodegradable polymers, in particular polyesters, have become sustainable alternatives to standard petroleum-based polymers in a growing number of demanding applications, and nowadays a variety of products are already in the market. Of all, probably poly(lactic acid) (PLA) is one of the biodegradable environmentally friendly polymers that more interest has attracted. However, some commercial applications of PLA are limited due to certain inferior properties such as brittleness, slow crystallization rate, and low melt viscosity. Alternatives, including preparations of composites and blending with other polymers, have been extensively investigated to overcome these drawbacks [1–6]. For instance, blends of PLA with soft biodegradable polyesters such as poly(butylene adipate-co-terephthalate) (PBAT) have been explored to extend its mechanical properties and fabricate more flexible materials

[7–10]. In fact, there already existing commercial products such as biodegradable, compostable, and partially biobased product Ecovio®, brand name of a polymer blend composed of 45 wt% of poly(lactic acid) (PLA) and 55 wt% of poly(butylene adipate-co-terephthalate), with applications in packaging, dual-use bags (shopping and waste) and agricultural films. Nevertheless, incorporation of fillers by preparing composites or nanocomposites is always a recurrent approach to overcome PLA based shortcomings, improve properties, or even add new functionalities [11,12].

In recent years, the use of zinc oxide fillers within PLA matrix has acquired great interest [13] due to their non-toxicity, availability, low cost and stability, and the properties that can impart to the materials such as high ultraviolet absorption capacity [14,15] and antimicrobial activity [16,17]. Moreover, ZnO and other Zn-based compounds also have a catalytic effect on the degradation of polyester matrices by depolymerization and intermolecular transesterification, especially at high temperatures [18,19]. However, the ZnO in nanoparticle form is considered as potential nanotoxic and European regulation avoids its use in products intended to be in contact with food or cosmetics. On the other hand, the use

\* Corresponding author.

E-mail address: [sbonilla@ictp.csic.es](mailto:sbonilla@ictp.csic.es) (A. Muñoz-Bonilla).

of microparticles having a hierarchical nanostructure is proven to provide an efficient antimicrobial response with low cytotoxicity due to a compromise between particle size and ROS generation mechanisms [20]. Thus, surface reactivity of nanomaterial is playing a predominant role in the interaction with organic substances.

The biodegradation of polymers included different degrees of material decomposition that combines several processes, mainly starts with a non-enzymatically hydrolysis that leads to a significant biodeterioration and/or biofragmentation accompanied with a molar weight reduction, followed by assimilation by microorganisms that further involves the enzymatic degradation [21,22]. The presence of functional particles, even nanoparticles, in the polymer matrix will be conditioning the biodegradation mechanisms and the synergetic effect could arise from particles that modulated its surface reactive as a consequence of the micro-nanostructure.

In term of polymer biodegradation, there is a wider variety of materials and environment that make difficult to assert the main mechanism. Among the different processes to eliminate the presence of urban solid waste, the industrial compost under controlled aerobic conditions is a biological decomposition process that completes the disintegration process in less than 90 days [23]. The enormous plastic and microplastic presence in urban waste such as in the case of landfill requires prolonged times to be decomposed. So, there is an urgent need to find an accelerated degradation process of plastic under controlled composting conditions. For such a reason, the research of the Zn-based compounds' effect on the degradation of biodegradable polyesters in different conditions has aroused a growing interest [24–26] and can contribute to accelerating the biodegradation process of such materials.

This work aims to elucidate the contribution of the ZnO compounds in the kinetics of the disintegration process under composting conditions of a biodegradable commercial polymer, Ecovio, which is a blend of poly(lactic acid) (PLA) and poly(butylene adipate-co-terephthalate) (PBAT). Different ZnO particles, in the nano and micro scale, are employed to investigate the ZnO size effect on the composite properties such as crystallinity, thermal degradability, and miscibility of the polymeric component. Moreover, the Ecovio-ZnO based composites and nanocomposites are further disintegrated under simulated composting conditions at the laboratory scale level to get information on how can ZnO size can influence the compostability of the Ecovio type biodegradable polymer.

## 2. Experimental part

### 2.1. Materials

Ecovio® F blend C2224, a biodegradable commercial blend composed by 55 wt% Ecoflex® (poly(butylene adipate-co-terephthalate), PBAT, containing 55% of aromatic segments) and 45 wt% poly(lactic acid) (PLA), was acquired from BASF (Germany). Technipol® 061/E, an aromatic-aliphatic copolyester was used as compatibilizers and obtained from Sipol (Italy). ZnO nanoparticles (NPZnO), and microstructured ZnO particles (MsZnO) were synthesized as previously described [27,28]. For comparative purposes two commercial ZnO reference particles were used, nanometric ZnO (nanoZnO) was purchased from Evonik industries (Germany) and micrometric ZnO (microZnO) was obtained from Asturiana de Cinc S.A. (Spain). Both materials were thermally treated at 500 °C to keep similar annealing conditions of synthesized ZnO.

### 2.2. Processing of biocomposites

Ecovio/ZnO composites were prepared by melt extrusion in an extruder equipped with twin conical co-rotating screws (MiniLab Haake Rheomex CTW5, Thermo Scientific) with a capacity of 7 cm<sup>3</sup>

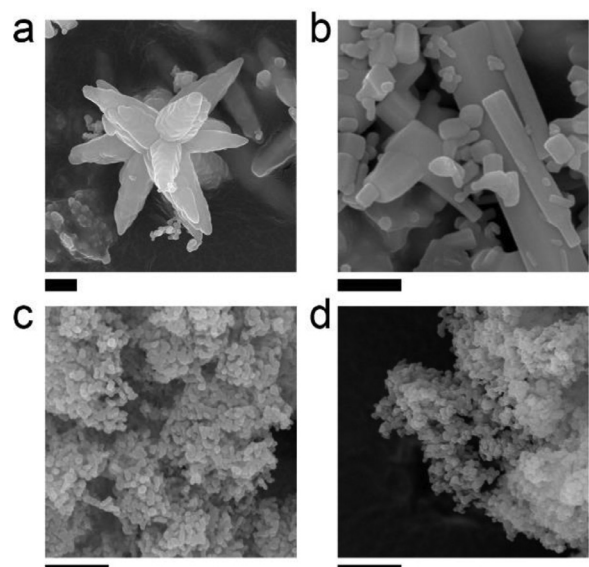


**Fig. 1.** Morphological characterization of the ZnO materials used as accelerating agents in the biodegradation process. FE-SEM of (a) microstructured ZnO (MsZnO) (b) commercial ZnO microparticles (microZnO) (c) synthesized ZnO nanoparticles (NPZnO) and, (d) commercial ZnO nanoparticles (nanoZnO). Scale bar, 500 nm.

at a screw speed of 100 rpm for 3 min at 180 °C. Ecovio (83 wt%) was loaded with the different types of ZnO particles (2 wt%) and Technipol compatibilizer (15 wt%). Prior to processing, all the materials were dried in an oven at 40 °C under vacuum for 24 h. Subsequently, the extruded composites and nanocomposites were compressed into films of about 200 μm using a Collin P200P press at 180 °C and 100 bars.

### 2.3. Disintegrability under composting conditions test

The disintegrability test under simulated composting conditions of the prepared samples was performed at laboratory scale level following the ISO 20,200 standard [23,29]. Several composite films of 15 mm × 15 mm size for each formulation were placed in textile meshes to allow contact with microorganisms and moisture, and also to permit their easy removal after composting test [30]. Then, the meshes were buried in a mixture of 45 wt% of solid synthetic wet waste (10% of compost (Compo, Spain), 30% rabbit food, 10% starch, 5% sugar, 4% corn oil, 1% urea, 40% sawdust) and 55 wt% of water contained in a perforated plastic box as composter reactors. The samples were subjected to an aerobic disintegration process, incubated at a controlled temperature of 58 °C. Samples of each formulation were withdrawn periodically, cleaned with distilled water, dried in an oven at 37 °C under vacuum for 24 h, and reweighed. The disintegration degree was calculated by normalizing the sample weight, at different days of composting, to the initial weight.

### 2.4. Characterizations

The morphology of the ZnO materials was evaluated by field emission scanning electron microscopy (FE-SEM, Hitachi S-4700). The distribution of the different blend components on the films was analyzed using confocal Raman microscopy on a CRM-Alpha 300 RA microscope (WITec, Ulm, Germany) equipped with Nd:YAG dye laser (maximum power output of 50 mW at 532 nm). Chemical analysis of the samples was also performed with a Hitachi SU8000 Scanning Electron Microscope equipped with an energy dispersive x-ray spectrometer (EDX) (Bruker Quantax 200). Molecular weights

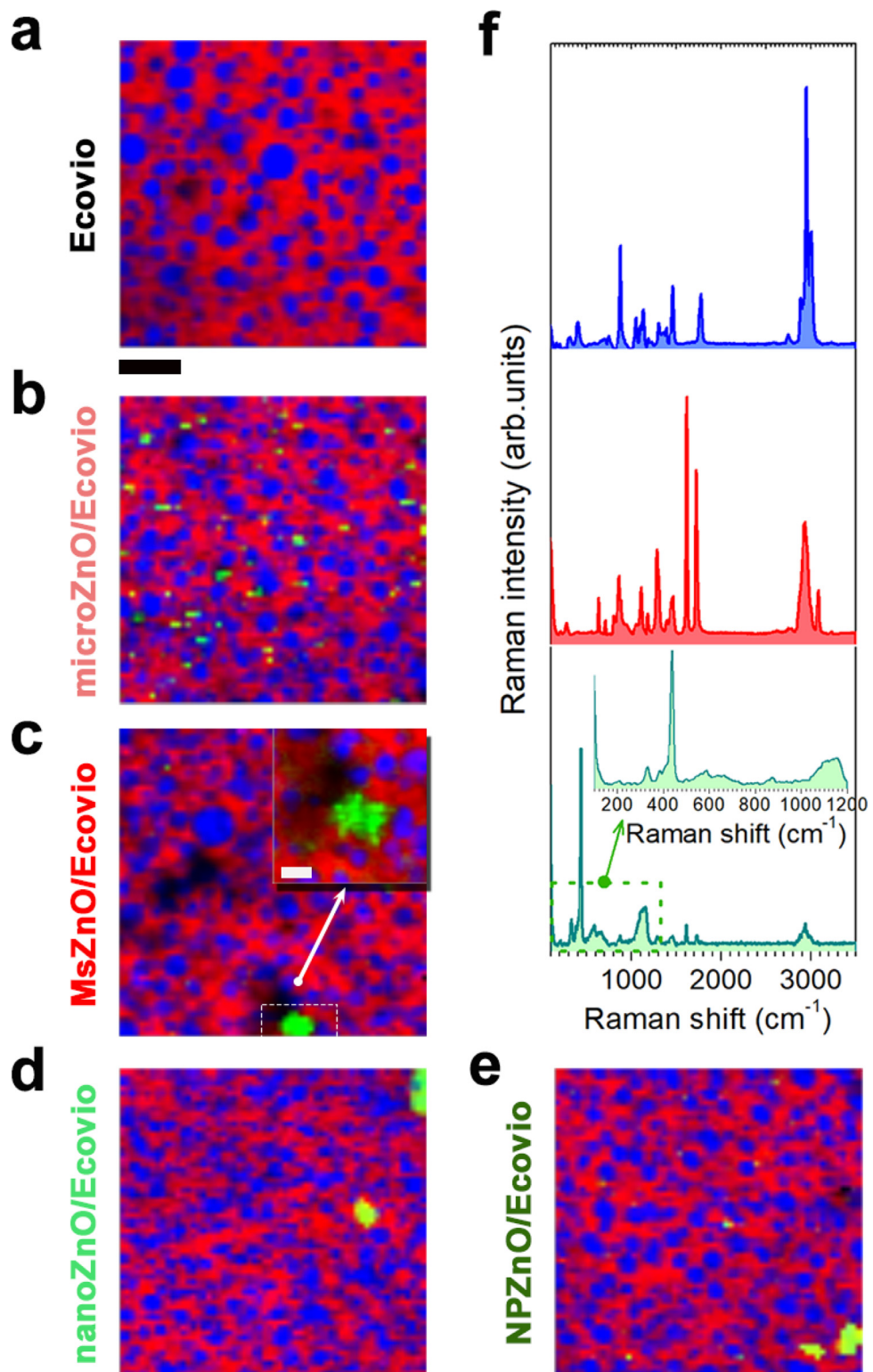


**Fig. 2.** Evaluation of the phase morphology of the Ecovio blend and its components. Raman micrographs (XY maps) of (a) Ecovio, (b) microZnO/Ecovio composite, (c) MsZnO/Ecovio composite, (d) nanoZnO/Ecovio composite and (e) NPZnO/Ecovio composite films. Average Raman spectra of the corresponding PLA (typical bands at 2947 cm<sup>-1</sup>, 1770 cm<sup>-1</sup>, 1454 cm<sup>-1</sup>, 393 cm<sup>-1</sup>), PBAT (bands at 1720 cm<sup>-1</sup> and 1615 cm<sup>-1</sup>) and a representative spectrum in which is clearly appreciated the band at 440 cm<sup>-1</sup> associated to the E<sub>2</sub> mode of ZnO materials. Blue: PLA, red: PBAT and green: ZnO particles. Scale bar in black, 10 μm, and scale bar in white, 3 μm. (For interpretation of the references to color in this figure legend, the reader is referred to the web version of this article.)

and polydispersity indexes of samples were determined by gel permeation chromatography (GPC) on Waters Division Millipore system equipped with a Waters 2414 refractive index detector using THF ( $1 \text{ mL min}^{-1}$  flow rate) as eluent at  $35^\circ\text{C}$ . The calibration was made with polystyrene standards (Polymer Laboratories LTD).

The films were thermally characterized by differential scanning calorimetry (DSC). The measurements were conducted on a TA Q2000 instrument (TA Instruments) under dry nitrogen ( $50 \text{ cm}^3 \cdot \text{min}^{-1}$ ). The samples were equilibrated at  $0^\circ\text{C}$  and heated to  $180^\circ\text{C}$  at  $10^\circ\text{C}/\text{min}$ . Then, a cooling scan from  $180^\circ\text{C}$  to  $0^\circ\text{C}$  and finally a heating scan from  $0^\circ\text{C}$  to  $200^\circ\text{C}$  was performed at the same rate. The glass transition temperatures ( $T_g$ ), cold crystallization temperatures ( $T_{cc}$ ), melting temperatures ( $T_m$ ), and the melting enthalpy ( $\Delta H_m$ ) were obtained from the first and second heating scan. Thermogravimetric analysis (TGA) of samples was performed on a TGA Q500 thermal analyzer (TA Instruments) at a heating rate of  $10^\circ\text{C} \cdot \text{min}^{-1}$  from  $40$  to  $800^\circ\text{C}$ , under air atmosphere ( $50 \text{ cm}^3 \cdot \text{min}^{-1}$ ). The instrument was calibrated both for temperature and weight by standard methods. Temperatures at the maximum degradation rate ( $T_{max}$ ) were calculated from the first derivative of the TGA curves (DTG). X-ray diffraction (XRD) measurements were performed using a Bruker D8 Advance instrument with a Cu K $\alpha$  source ( $0.154 \text{ nm}$ ) and a detector Vantec1. The scanning range was  $4^\circ$ – $40^\circ$ , step-size  $0.023851^\circ$ , and count time per step  $0.2 \text{ s}$ .

### 3. Results and discussion

In this current work, micro and nano ZnO materials, MsZnO and NPZnO, respectively, previously developed and characterized [27,28] were evaluated as fillers in biodegradable composites and compared with reference commercial materials, nanoZnO, and microZnO. Fig. 1 displays the different morphologies of the ZnO materials used in this study, which all present the wurtzite hexagonal structure, typical of ZnO. FE-SEM micrographs show the multidomain ZnO microparticles (MsZnO) with a star-shaped morphology and particle size of around  $1.5 \mu\text{m}$  (Fig. 1a), whereas the main morphology of commercial microZnO is hexagonal rods with lengths of  $1 \mu\text{m}$  (Fig. 1b). Related to the nanometric materials, both samples are characterized as large aggregates of primary ZnO nanoparticles with diameters of around  $56 \text{ nm}$  and  $20 \text{ nm}$ , for synthesized NPZnO (Fig. 1c) and commercial nanoZnO (Fig. 1d) materials, respectively.

Then, Ecovio-based composites films (thickness of about  $200 \mu\text{m}$ ) filled with 2 wt% of the different ZnO materials were prepared by melt extrusion followed by compression molding. The resulting films were analyzed by Raman confocal microscopy to evaluate the phase morphology of the Ecovio blend and their composites. Fig. 2 shows Raman micrographs (XY maps) of the films and the corresponding spectra of the different components of Ecovio, i.e. PLA (in blue color) and PBAT (in red color), and ZnO particles (in green color). The micro-Raman mapping were performed by taking spectra point by point with a step of  $100 \text{ nm}$ , and using the signal at  $1770 \text{ cm}^{-1}$  of PLA, the strong band at  $1615 \text{ cm}^{-1}$  attributed to PBAT and the signal of the ZnO at  $440 \text{ cm}^{-1}$ . The color regions represent the higher intensity integrated for each bands. It is clearly observed the phase-separated microstructure of the Ecovio blend, with two main regions, PLA-rich quasi-spherical microdomains (blue areas) homogeneously dispersed on PBAT-rich continuous phase matrix (red areas). In the composites samples containing the different ZnO materials as filler, few small particle aggregates of ZnO nanoparticles can be also identified (green colors) in these  $50 \times 50 \mu\text{m}$  mappings, whereas individual microparticles can be identified in Fig. 2b and 2c. Remarkably, the PLA domains in these composite samples are smaller when compared to the neat Ecovio blend, especially in the composites con-

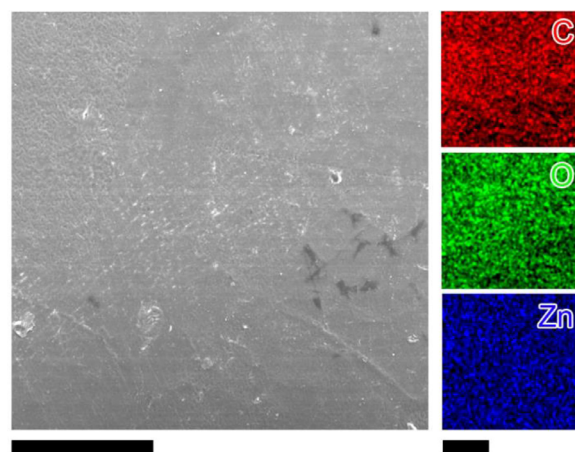


**Fig. 3.** Evaluation of the compositional homogeneity. SEM image of MsZnO/Ecovio composite material, and its corresponding element mapping distributions of C, O, and Zn. Scale bar,  $200 \mu\text{m}$ .

taining nanometric particles (Fig. 2d and 2e). The mean diameters of the PLA domains determined from the images were found to be  $2.5 \pm 0.8 \mu\text{m}$  for Ecovio,  $1.9 \pm 0.7 \mu\text{m}$  for MsZnO/Ecovio composite,  $1.9 \pm 0.6 \mu\text{m}$  for microZnO/Ecovio composite,  $1.9 \pm 0.5 \mu\text{m}$  for NPZnO/Ecovio composite and  $1.7 \pm 0.5 \mu\text{m}$  for nanoZnO/Ecovio composite. This fact seems to indicate that the ZnO particles could act as nucleating agents of PLA crystals thus; more and smaller PLA domains are formed, which can be better dispersed in the PBAT matrix. This also suggests a uniform distribution of the ZnO particles in the polymer blend in spite of the aggregates observed in Raman images.

SEM-EDX elemental analysis was also performed to evaluate the dispersion of the filler in the polymer blend. As an example, Fig. 3 displays the EDX mapping of the MsZnO/Ecovio composite which reveals the uniform C, O, and Zn elemental distribution, thereby a homogenous dispersion on the macroscale of the load.

DSC analysis was used to investigate the thermal behavior and the crystallization behavior of the Ecovio based biocomposites containing micro and nanometric ZnO particles. The curves of the first and second heating scan are displayed in Fig. 4 while the parameters including glass transition ( $T_g$ ), cold crystallization ( $T_{cc}$ ), and melting temperatures ( $T_m$ ) are summarized in Table 1. The second run will allow us to determine the miscibility of blends. In all the samples, it is clearly observed the  $T_g$  of PLA at around  $60^\circ\text{C}$ , confirming the immiscibility between PBAT and PLA as described [7] even with the incorporation of Technipol compatibilizer. The  $T_g$  values of the composites were not significantly different compared to Ecovio; therefore, the incorporation of particles does not pointedly alter this immiscibility. This Ecovio blend presents a cold crystallization temperature at  $83^\circ\text{C}$  and a melting process at ca.  $105^\circ\text{C}$ , corresponding to Technipol, which is clearly observed in the first heating run. This cold-crystallization is diminished by the presence of particles in the blend, suggesting that the particles are able to crystallize Technipol during film processing.

The PBAT showed two broad endothermic peaks around  $50$  and  $120^\circ\text{C}$ . These double melting peaks are attributed to recrystallization process [31,32]. The lower melting peak arises from original crystals, while the higher one arises from recrystallization during heating. Then, for the Ecovio blends, there was an overlapping between the Technipol, PBAT melting region, and the PLA cold-crystallization region [9,10,33]. For this reason, it was not possible to establish the PBAT melting temperature in the materials and only PLA melting was determined. Depending on the processing conditions PLA also showed a double endothermic peak at around  $150^\circ\text{C}$  and  $153^\circ\text{C}$  due to a recrystallization mechanism typical

**Table 1**

Main thermal parameters, glass transition temperature ( $T_g$ ), cold crystallization temperature ( $T_{cc}$ ), melting temperature ( $T_m$ ) and melting enthalpy ( $\Delta H_m$ ) obtained by DSC during the first and second heating runs.

Sample	First run				Second run				$\Delta H_m$ (J/g)	
	$T_{gPLA}$ (°C)	$T_{ccPLA}$ (°C)	$T_{mPLA}^1$ (°C)	$T_{mPLA}^2$ (°C)	$\Delta H_m$ (J/g)	$T_{gPLA}$ (°C)	$T_{ccPLA}$ (°C)	$T_{mPLA}^1$ (°C)	$T_{mPLA}^2$ (°C)	
Ecovio	61	121	149	—	8.1	59	—	151	—	3.3
nanoZnO/Ecovio	56	113	146	154	12.4	58	119	147	154	12.6
NPZnO/Ecovio	57	117	148	155	11.8	59	126	149	155	10.5
microZnO/Ecovio	60	116	148	154	10.9	58	129	151	154 <sup>a</sup>	8.7
MsZnO/Ecovio	56	121	149	154 <sup>a</sup>	8.6	59	128	150	154 <sup>a</sup>	8.3

<sup>a</sup> appears as a shoulderThe errors of the temperature and enthalpy values are equal to  $\pm 1$  and  $\pm 0.1$ , respectively.

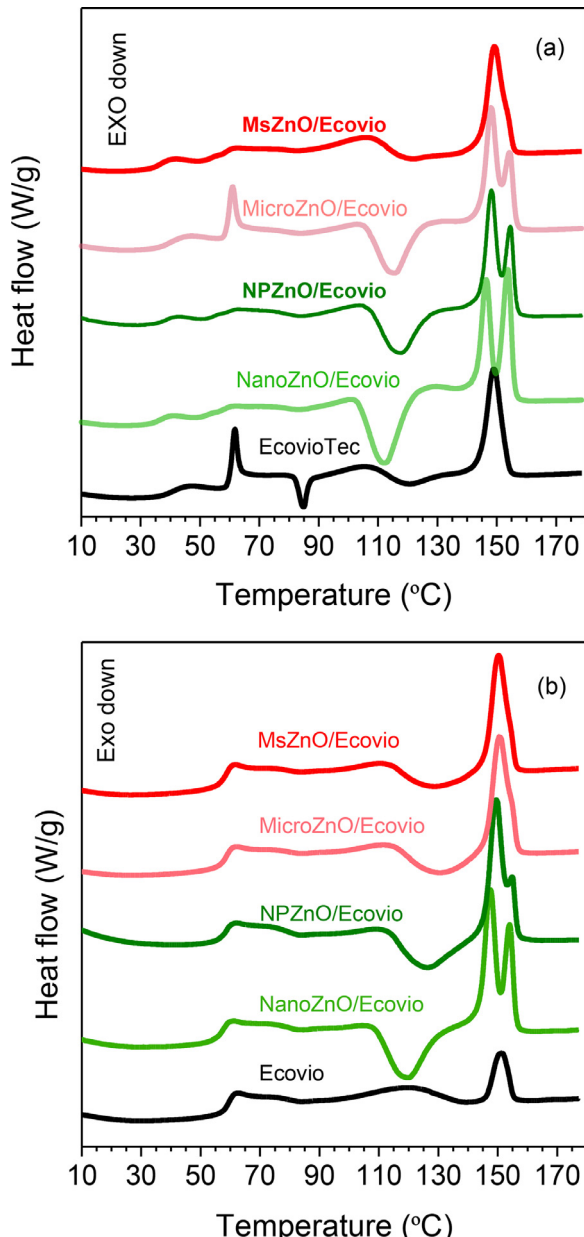


**Fig. 4.** Determination of the main thermal parameters of the composite films. DSC curves of the first (a) and second (b) heating scan of Ecovio and MsZnO/Ecovio, microZnO/Ecovio, NPZnO/Ecovio, nanoZnO/Ecovio composite films.

for polyesters [7,34]. Cold crystallization is more evident in the composite samples, meaning that the DSC cooling conditions did not allow the complete crystallization of PLA and, thus, the ZnO fillers favor the crystallization of PLA upon DSC second heating. The  $T_{cc}$  slightly shifts to lower temperatures in composites with

ZnO particles in the nanoscale compared to that of the micrometric fillers. Moreover, the ZnO particles in the nanoscale intensified the  $T_{cc}$  indicating that they avoid the complete crystallization of PLA nanocomposites in the processing step and thus PLA crystallizes during DSC heating. Then, an abroad single melting peak (149 °C) was observed for the Ecovio blend without particles. Whereas, the melting curves of nanocomposite samples clearly show bimodal peaks at 140–160 °C, which correspond to two different types of crystal caused by the formation of small and imperfect crystals [35] that further change into more stable through melting and recrystallization. Although in composites containing ZnO microparticles, MsZnO, and microZnO, the two melting peaks are not as clear, a small shoulder appears at higher temperatures, also indicating the formation of small amounts of imperfect crystallites with a bimodal size distribution. The crystallization temperature ( $T_c$ ) upon cooling increases in the composites samples compared to the neat Ecovio, which also indicates a possible nucleation effect of the ZnO particles. The Ecovio blend presents a  $T_c$  of 84 °C, while the  $T_c$  of the composites samples were found to be 86, 87, 87 and 86 °C, for microZnO/Ecovio, MsZnO/Ecovio, nanoZnO/Ecovio and NPZnO/Ecovio, respectively.

Therefore, the nucleation effect of the ZnO fillers previously deduced from the Raman microscopy analysis of the samples is now confirmed by calorimetry; in particular in the nanocomposite samples, in which a more homogeneous dispersion in the polymeric blend is achieved.

The thermal stability of the prepared composites was studied by TGA. The thermograms of the Ecovio and ZnO/Ecovio biocomposite films are graphically presented in Fig. 5 and the thermal parameters summarized in Table 2. Ecovio blend shows three steps decomposition processes under air atmosphere, the first step associated with the PLA phase ( $T_{dmax}^1 = 356$  °C), and the second and third steps assigned to the decomposition of PBAT ( $T_{dmax}^2 = 401$  °C and  $T_{dmax}^4 = 518$  °C, respectively) [8]. Remarkably, the incorporation of only 2 wt% of ZnO nanoparticles drastically changes the thermal degradation behavior; the thermal stability of the biocomposites is considerably lowered in all the cases. This reduced thermal stability in the presence of ZnO particles observed previously in other works [17,19,25,36,37] may be due to the catalytic effect of ZnO particles in degradation reactions such as intermolecular transesterification reactions and depolymerization [18]. The decomposition temperatures at 10% weight loss ( $T_{d10}$ ), and the temperatures of the maximum rate of weight loss for each step shift to lower values in the samples containing ZnO particles. Notice that also degradation steps associated with the PBAT phase also shift to lower temperatures, suggesting that ZnO particles could also affect the thermal stability of this polymer. Simultaneously, an additional decomposition step at around 390 °C is appreciated in the biocomposites, ending with four main steps of degradation processes. This additional process has been previously observed in other ZnO/PLA composites and attributed to the decomposition of polymer adsorbed on ZnO surfaces [18,38,39]. The char residue was found to be around 2 wt% for all the

**Table 2**

Thermal degradation parameters: decomposition temperatures at 10% weight loss ( $T_{d10}$ ), temperatures of the maximum rate of weight loss for each step ( $T_{dmax}^1$ ,  $T_{dmax}^2$ ,  $T_{dmax}^3$ , and  $T_{dmax}^4$ ) and their corresponding derivative weight (%/ °C).

Sample	$T_{d10}$ ( °C)	$T_{dmax}^1$ ( °C)	$dT/dw^1$ (%/ °C)	$T_{dmax}^2$ ( °C)	$dT/dw^2$ (%/ °C)	$T_{dmax}^3$ ( °C)	$dT/dw^3$ (%/ °C)	$T_{dmax}^4$ ( °C)	$dT/dw^4$ (%/ °C)
Ecovio	339	356	1.16	401	1.52			518	0.13
nanoZnO/Ecovio	255	270	0.75	367	0.86	389	0.65	468	0.13
NPZnO/Ecovio	249	263	0.84	366	0.78	392	0.68	473	0.13
microZnO/Ecovio	261	277	0.83	365	0.95	393	0.70	476	0.16
MsZnO/Ecovio	279	290	1.06	371	0.97	394	0.64	480	0.15

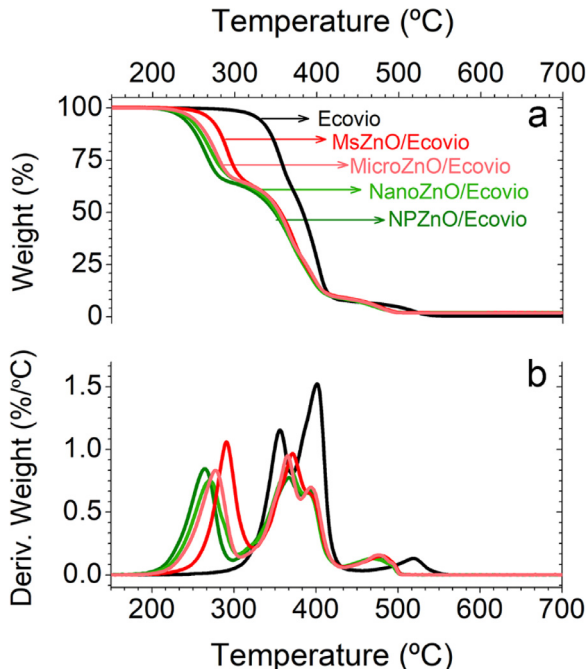


**Fig. 5.** (a) Thermogravimetric analysis and (b) derivative thermogravimetric curves of neat Ecovio and Ecovio/ZnO biocomposites.

biocomposites in agreement with the ZnO loading, confirming the high thermal stability of ZnO.

Therefore, the TGA study revealed the catalytic effect of ZnO particles in the thermal degradation of Ecovio during the heating under air atmosphere, which is more pronounced when the ZnO nanoparticles are in the nanoscale, may be due to the larger surface area in contact with the polymeric matrix. The catalytic effect of ZnO on thermal and hydrolytic degradation in PLA/ZnO composites has been extensively evaluated under different experimental conditions [24,38]. However, its effect on composites' disintegration when exposed to the composting environment has been not studied before to the best of our knowledge. In the current work, the prepared Ecovio/ZnO biocomposites were disintegrated under composting conditions (58 °C, 50% of humidity and in aerobic conditions) at laboratory scale-level to evaluate their compostability and their potential as sustainable end-life material. Fig. 6 shows the visual appearance of composite films recovered at different times of disintegration in compost. During the first week of composting, all the films slightly deform, turn yellowish, and their opacity increases. These changes are signal of water absorption and the formation of low molecular weight compounds due to the hydrolytic degradation process [30,40]. The color of the compost medium also changed becoming dark brown in 1 week (Fig. 6-f), accompanied with ammonia odor as establish the ISO 20,200 standard [23]. Then, over the composting the color of the films changes from yellowish, brown to dark brown. Meanwhile, the

compost medium ultimately results in humus-rich soil confirming the successful of the disintegration process mediated by the thermophilic microorganisms [30,40]. Remarkably, the disintegration test demonstrates that ZnO composite materials degrade noticeably faster than neat Ecovio blend, especially the sample with star-shaped ZnO microparticles (MsZnO) in which high fragmentation is clearly appreciated after 21 days.

The film's disintegrability was also evaluated in terms of mass loss as a function of composting time (see Fig. 7). Likewise, it can be seen that ZnO fillers significantly accelerate the degradation process during the first 21 days. Afterward, the composite containing star-shaped ZnO microparticles (MsZnO) leads to a noticeably improved degradation rate in comparison with the neat Ecovio blend, although higher degradation levels are appreciated in all the composite samples. Indeed, this difference in the disintegration behavior can be ascribed to the catalytic effect of ZnO on the hydrolytic degradation of the blend. However, the surface areas in contact with ZnO fillers related to their particle size seem to be not relevant in the polymer degradation rate. In fact, the biggest particles, MsZnO microparticles, allow faster degradation of the blend. Then, another mechanism might be also implied in the degradation of Ecovio.

It is reported that the degradation of PBAT under composting conditions is considerably slower than that of PLA [41,42]. While PLA almost degrades at 16 days, much longer incubation time is required to degrade PLA/PBAT blends and PBAT [29]. Then, from the results obtained in the disintegration test, it can be said that the first degradation step in which the effect of ZnO filler is more evident, would be more related to the PLA phase, since in 32 days under composting neat PLA reach more than 95% of mass loss [6]. Samples taken at different incubation time in compost were further analyzed Confocal Raman microscopy.

In effect, from Raman images (Fig. 8) it is clear that the blue regions representing the PLA phase tend to disappear from the first days of composting, meaning that phase PLA degrades faster than PBAT as expected. It is also appreciated that the ZnO fillers accelerate the degradations of PLA in comparison with the films obtained from neat Ecovio. Fig. 9 displays the variations observed in the average Raman spectra of the Ecovio and composites samples recovered at different incubation times in compost. After the first days in compost, it is observed a notably decrease in the relative intensity of the main bands associated to PLA, e.g. at 1770 cm<sup>-1</sup> ( $\nu$  C=O), 1454 cm<sup>-1</sup> ( $\delta$  CH<sub>3</sub>), 1130 cm<sup>-1</sup> ( $r_s$  CH<sub>3</sub>) and 393 cm<sup>-1</sup> ( $\delta$  CCO); related to the bands assigned to PBAT, 1720 cm<sup>-1</sup> ( $\nu$  C=O) and 1615 cm<sup>-1</sup> ( $\nu$  C=C in benzene ring). This decrease on the relative intensity is higher in samples with ZnO particles, suggesting that the ZnO fillers favor the degradation of PLA.

However, no evidence of ZnO particles is found in the films after only 7 days under compost conditions, even when films did not show evident physical disintegration (Fig. 6). Nevertheless, from Fig. 7 is evident that films lost considerable amount of mass (around 15%) during the first week of composting with the exception of neat Ecovio film. The samples taken at 7 days of composting were further analyzed by XRD experiments and compared with the films obtained as prepared (Fig. 10).

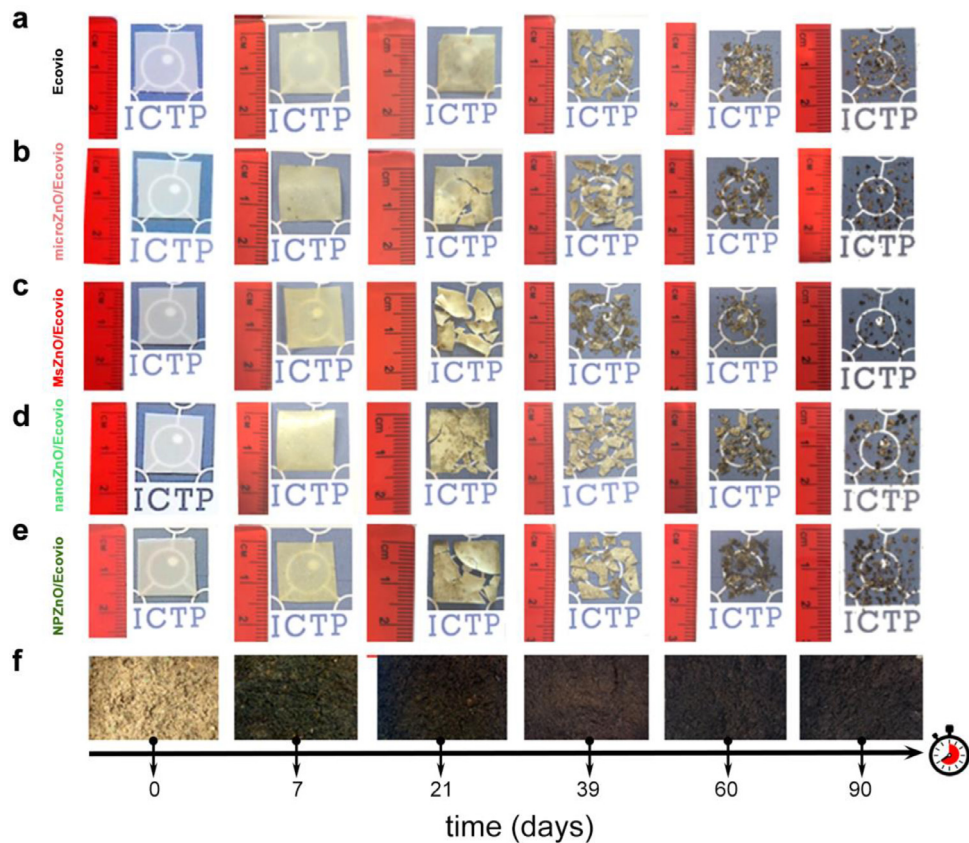


**Fig. 6.** Photographs of neat Ecovio and composite films recovered at different incubation times in composting conditions (to highlight the loss of transparency and the fragmentation of the polymer films, they have been photographed on the top of blue ICTP-CSIC logo). (For interpretation of the references to color in this figure legend, the reader is referred to the web version of this article.)

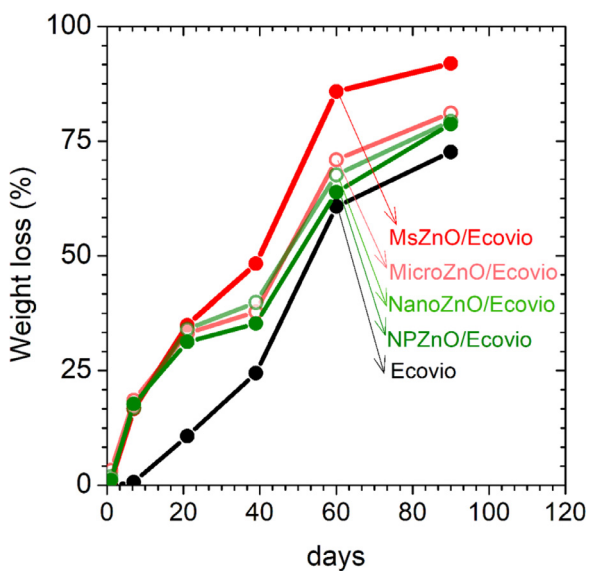


**Fig. 7.** Disintegration curves under composting conditions of Ecovio and composite films.

The patterns of all films before composting display an amorphous halo corresponding to the amorphous phase of the polymers, in accordance with the first DSC heating scan, and the main diffraction peaks of PBAT at  $2\theta = 16.3^\circ$ ,  $17.6^\circ$ ,  $20.4^\circ$ ,  $23.1^\circ$ , and  $25.0^\circ$ , assigned to planes (011), (010), (101), (100), and (111), respectively [7]. The diffraction peaks of PLA are not clearly observed in the neat composites (0 days), due to the mainly amorphous character

of the films. Also, in composite films appear the peaks attributed to the ZnO particles at  $2\theta = 31.8$  (100),  $34.5$  (002),  $36.5$  (101), and  $47.6$  (102). From the patterns of the films at 7 days in compost, it is evident that the peaks corresponding to ZnO particles completely disappear. It seems that particles are chemically dissolved releasing  $Zn^{2+}$  ions into the compost medium and they are subjected to alterations through interactions with naturally occurring biomacromolecules or geomacromolecules including proteins, polysaccharides, and humic substances [43–45].

On the other hand, two strong peaks associated with the PLA at  $2\theta = 16.8^\circ$  due to diffraction from (110)/(200) and at  $19.0^\circ$  attributing to reflections of the (203) plane [46,47] appear in the pattern. This change implies the increase of the ratio of the crystalline-to-amorphous region because the compost was maintained at temperatures slightly over the PLA  $T_g$  that served to enhance the crystallization. In addition, the amorphous phase degraded more rapidly than crystalline regions, also contributing to an increase in the percentage of the crystalline phase. As XRD measurements confirmed the loss of ZnO particles at the beginning of the disintegration process in compost, the chemical composition of the films was then investigated by SEM-EDX elemental analysis. Table 3 summarizes the compositional results of the MsZnO/Ecovio composite films as prepared and in the soil after 7 days of composting. Similarly, the measurements confirm not only the disappearance of ZnO particles but also the absence of Zn atoms after only 7 days in compost. Besides, the content of oxygen augments due to the hydrolytic degradation of the polymer. The PLA disintegrability starts by the PLA hydrolysis process, followed of the microorganisms attack by eroding the polymer surface [22]. Thus, the presence of nitrogen in the 7 days disintegrated composite film can be an indicative of the microorganisms' erosion process, as microorganisms use nitrogen

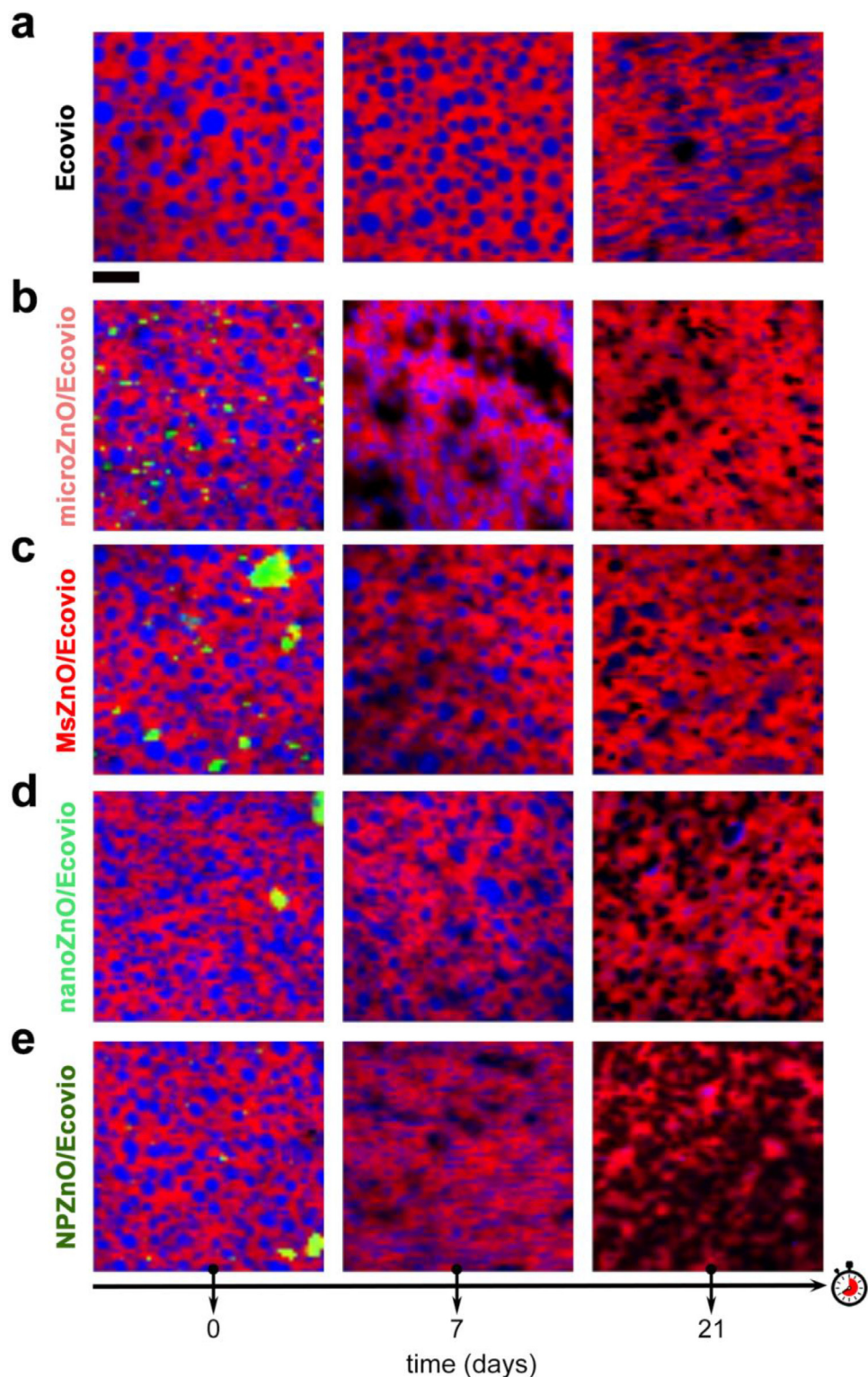


**Fig. 8.** Raman images of Ecovio, ZnO/Ecovio composites recovered at different incubation times in compost. Blue: PLA, red: PBAT, and green: ZnO particles. Scale bar, 10  $\mu$ m. (For interpretation of the references to color in this figure legend, the reader is referred to the web version of this article.)

as source for building cells [48]. The presence of nitrogen in the samples at this stage of the composting test is in good agreement with the already commented ammonia odor of the composting reactors.

The samples were further analyzed by GPC to study the molecular weight evolution during the first stages of degradation. **Table 4**

summarized the number average molecular weights and the polydispersity indexes (relative values calculated based on PS calibration) of Ecovio and composites samples recovered at different incubation times in compost (0, 7 and 21 days).

First of all, it is evident the ZnO particles exert a catalytic effect on the degradation of Ecovio during melt mixing

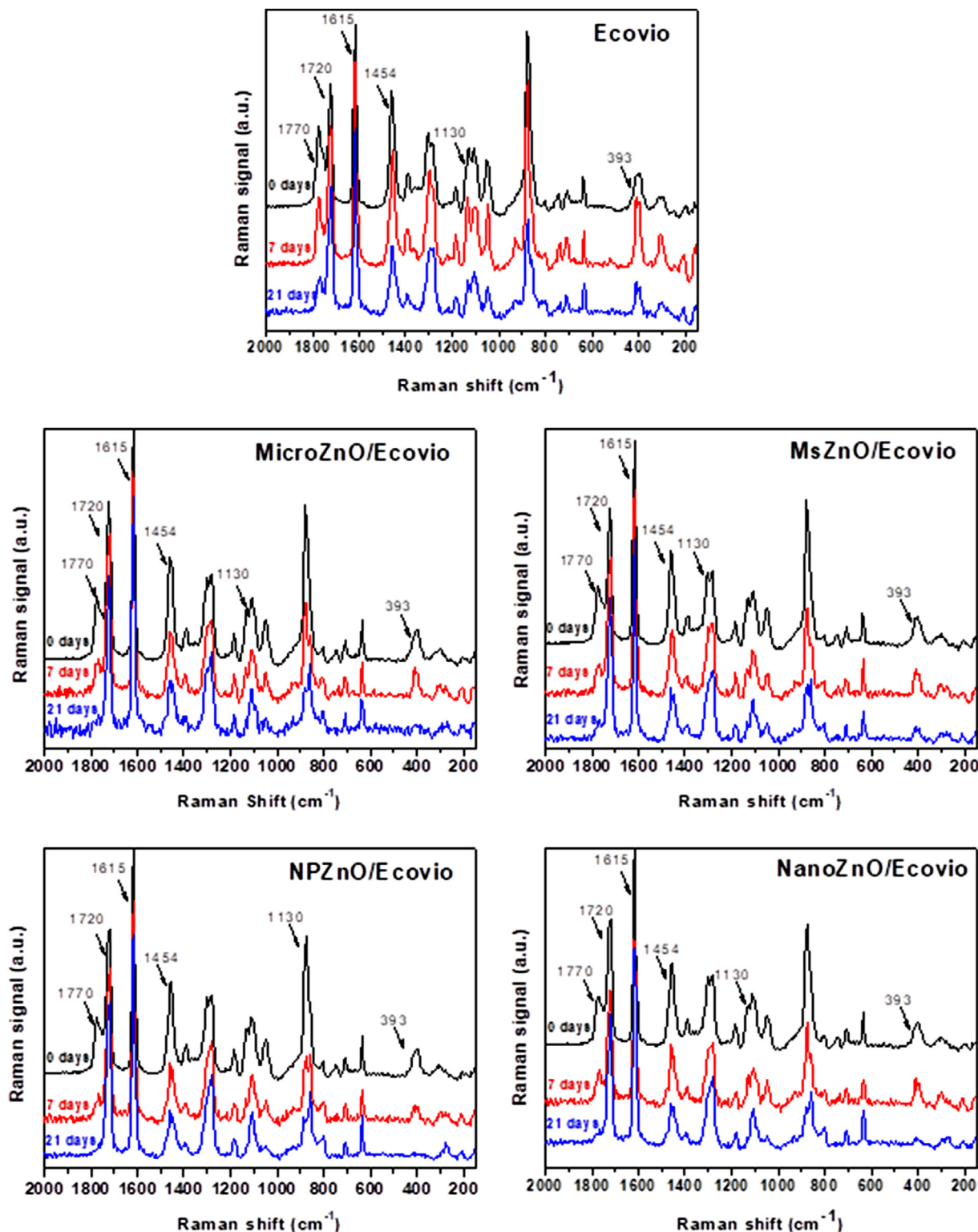


**Fig. 9.** Average Raman spectra of Ecovio, ZnO/Ecovio composites recovered at different incubation times in compost.

and processing steps. The composites samples show a significant reduction in the molecular weight in comparison with the Ecovio blend after melt-extrusion and compression molding (0 days). Remarkably in the sample containing MsZnO particles, this reduction in the molecular weight is smaller, probably due to the smaller surfaces area of ZnO particles in contact with polymeric phase. After 7 days in compost, the molecular weight dramatically de-

creases in all the samples, also in the MsZnO/Ecovio composite. The reduction for the next days of compost incubations tends to be slighter, as previously reported for the degradation of PLA and PLA composites samples, in which a rapid decrease of the molecular weight is observed during first days followed by a plateau phase of nearly constant molecular weight at least until 24 days in compost [47].

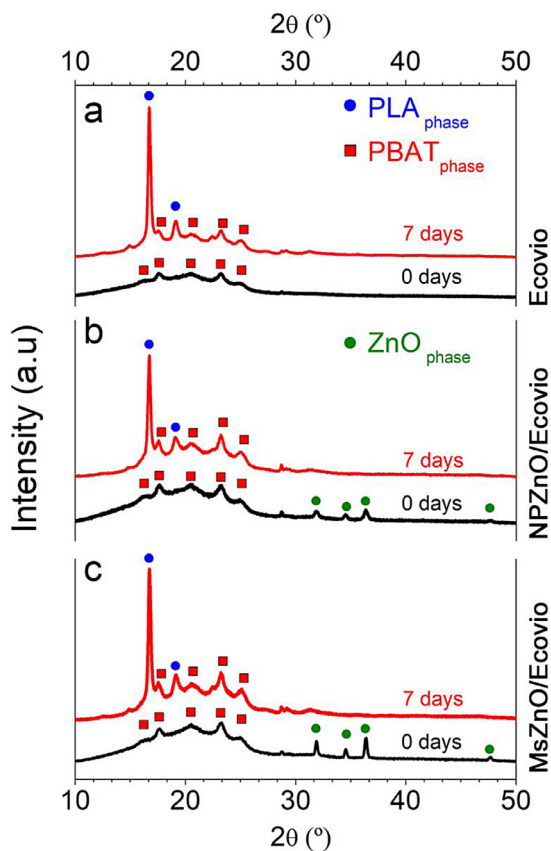


**Fig. 10.** XRD patterns of a) Ecovio, b) NPZnO/Ecovio, and c) MsZnO/Ecovio at 0 and 7 days in compost.

**Table 3**

Elemental quantitative data representative of the sample MsZnO/Ecovio composite film as prepared (0 days) and in soil (after 7 days in composting).

Element	0 days		7 days	
	Weight (%)	Atomic (%)	Weight (%)	Atomic (%)
C	58.95	66.58	56.03	62.72
O	39.11	33.11	41.19	34.62
Zn	1.94	0.40	—	—
N	—	—	2.78	2.67

**Table 4**

Number average molecular weights ( $M_n$ ) and polydispersity indexes (PDI) of neat Ecovio and composite films recovered at different incubation times in composting conditions.

Sample	0 days		7 days		21 days	
	$M_n$ (g/mol)	PDI	$M_n$ (g/mol)	PDI	$M_n$ (g/mol)	PDI
Ecovio	63,800	2.33	17,900	2.13	13,900	2.27
nanoznO/Ecovio	42,800	2.38	16,100	2.44	12,500	1.98
NPZnO/Ecovio	43,000	2.78	16,700	2.38	12,000	2.20
microZnO/Ecovio	42,100	2.47	16,200	2.54	11,000	2.61
MsZnO/Ecovio	53,500	2.82	16,000	2.49	12,700	2.19

From the results obtained in this work, it can be said that ZnO particles clearly accelerate the disintegration process of the Ecovio polymeric blend. However, it seems that the particles exert their effect on the polymer degradation only at the initial stages (less than 7 days in compost), initiating or advancing some hydrolytic reactions, as no signal of ZnO were found after 7 days of composting in the tested conditions. This effect is more pronounced in the case of multidomain ZnO microparticles (MsZnO) with a star-

shaped morphology and negative charge accumulation in localized regions of the structure [27]. As the micrometric particles possess a lower specific surface area, the dissolution in the acid environment of the compound would require a longer time. The hydroxylation of the surface of ZnO could assist the hydrolysis of PLA adsorbed on the ZnO surface [38] and, the longer the presence of ZnO, the faster the degradation of the polymer chain. This process is also favored by the compost temperature that it is slightly higher than the glass transition temperature ( $T_g$ ) of PLA in which the hydrolytic degradation of PLA is also accelerated.

It is worth to mention that the biodegradation of the sample MsZnO/Ecovio composite film reaches >90% (frequently used as the goal of samples disintegrability under composting [30,40]), in just 90 days which is according to the ISO 20,200 standard the maximum disintegration time allowed under the thermophilic composting conditions used here and thus suggesting that the materials did not require further mesophilic disintegration conditions. So, a reduction of more than 50% in time is accomplished by the use of nanostructured microparticles having accumulated negative charge at their surface. The photocatalytic effect of ZnO nanoparticles under UV excitation is suggested to initiate the radical oxidation of PLA [49]. In the present work, the composting was kept under dark conditions, so the appearance of negative charges at the surface of the ZnO crystal structure is not promoted by the photon-exciton appearance. Although further studies are required to shorten the biodegradation by using functional microparticles oxides with tailored surface properties, the charged star-shaped ZnO microparticles present the potential to accelerate the disintegration process of commercial PLA-PBAT blends.

#### 4. Conclusions

Composites based on biodegradable Ecovio polymer loaded with different ZnO particles (2 wt%) were successfully prepared by melt extrusion followed by compression molding. Raman confocal microscopy demonstrated that the incorporation of ZnO particles as filler contributes to improving the homogeneity of the Ecovio blend. The PLA microdomains dispersed on PBAT continuous phase are remarkably smaller in the samples with ZnO particles, especially in the case of nanometric particles, probably due to a nucleating effect of the particles. This effect was also evidenced by DSC, which showed that ZnO fillers favor the crystallization of PLA upon heating although the formation of crystallites with a bimodal size distribution. The incorporation of nanoparticles also provokes drastic changes in the thermal degradation behavior of the composites; again the stability is more affected when nanometric particles are employed. The modifications that ZnO fillers impart to the Ecovio polymer together with the catalytic effect of the ZnO particles also influence the biodegradability of the composites. The disintegration of the composites was evaluated in a simulated composting environment at laboratory scale level. Remarkably, ZnO composite materials degrade markedly faster than neat Ecovio blend, in particular in the first steps of the process. This effect is particularly evident in the sample with star-shaped ZnO microparticles, the biggest particles in size used in this study, suggesting that the particle size seems to be not relevant in the polymer degradation rate. Further studies of the degraded samples performed by Raman microscopy and XRD demonstrated that the PLA component degrades faster than PBAT, thus these results seem to indicate that the ZnO fillers mostly affect to PLA phase at the beginning of the degradation process. Indeed, no signal of ZnO particles was found in the samples after only 7 days under compost conditions, suggesting that the ZnO is dissolved relatively rapidly from the composite surface. It is worth pointing out that this stimulant behavior observed here could have potential technological applications such as accelerator in the disintegration of compostable polymers.

## Credit author statement

Due to the sensitive nature of the questions asked in this study, survey respondents were assured raw data would remain confidential and would not be shared.

## Declaration of Competing Interest

The authors declare that they have no known competing financial interests or personal relationships that could have appeared to influence the work reported in this paper.

## Acknowledgement

This research was funded by the [MICINN](#) under the projects [PID2019-104600RB-I00](#) and [MAT2017-86450-C4-1-R](#), the [Spanish National Research Council](#) (CSIC) under the project [NANOMIND](#) CSIC 201560E068, the [Agencia Estatal de Investigación](#) (AEI, Spain), and [Fondo Europeo de Desarrollo Regional](#) (FEDER, EU). F.R.-M is indebted to MINECO for a 'Ramon y Cajal' contract (ref: Ryc-2015-18626), which is co-financed by the [European Social Fund](#). F.R.-M also acknowledges support from a 2018 Leonardo Grant for Researchers and Cultural Creators (BBVA Foundation).

## References

- [1] J.-M. Raquez, Y. Habibi, M. Murariu, P. Dubois, Polylactide (PLA)-based nanocomposites, *Prog. Polym. Sci.* 38 (2013) 1504–1542.
- [2] L. Peponi, V. Sessini, M.P. Arrieta, I. Navarro-Baena, A. Sonseca, F. Dominicí, et al., Thermally-activated shape memory effect on biodegradable nanocomposites based on PLA/PCL blend reinforced with hydroxyapatite, *Polym. Degrad. Stab.* 151 (2018) 36–51.
- [3] A. Sonseca, S. Madani, G. Rodriguez, V. Hevilla, C. Echeverría, M. Fernández-García, et al., Multifunctional PLA blends containing chitosan mediated silver nanoparticles: thermal, mechanical, antibacterial, and degradation properties, *Nanomaterials* (Basel) (2019) 10.
- [4] K. Skrlova, K. Malachova, A. Munoz-Bonilla, D. Merinska, Z. Rybkova, M. Fernández-García, et al., Biocompatible Polymer Materials with Antimicrobial Properties for Preparation of Stents, *Nanomaterials* (Basel) 9 (2019) 1548.
- [5] C. Echeverría, A. Muñoz-Bonilla, R. Cuervo-Rodríguez, D. López, M. Fernández-García, Antibacterial PLA fibers containing thiazolium groups as wound dressing materials, *ACS Appl. Bio Mater.* 2 (2019) 4714–4719.
- [6] M.P. Arrieta, L. Peponi, D. López, M. Fernández-García, Recovery of yerba mate (*Ilex paraguariensis*) residue for the development of PLA-based bionanocomposite films, *Ind. Crops. Prod.* 111 (2018) 317–328.
- [7] L.C. Arruda, M. Magatón, R.E.S. Bretas, M.M. Ueki, Influence of chain extender on mechanical, thermal and morphological properties of blown films of PLA/PBAT blends, *Polym. Test.* 43 (2015) 27–37.
- [8] S. Xiang, L. Feng, X. Bian, G. Li, X. Chen, Evaluation of PLA content in PLA/PBAT blends using TGA, *Polym. Test.* 81 (2020) 106211.
- [9] R. Muthuraj, C. Lacoste, P. Lacroix, A. Bergeret, Sustainable thermal insulation biocomposites from rice husk, wheat husk, wood fibers and textile waste fibers: elaboration and performances evaluation, *Ind. Crops. Prod.* 135 (2019) 238–245.
- [10] D. Lascano, L. Quiles-Carrillo, R. Balart, T. Boronat, N. Montanes, Toughened Poly(Lactic Acid)-PLA formulations by binary blends with poly(Butylene Succinate-co-Adipate)-PBSA and their shape memory behaviour, *Materials* (Basel) 12 (2019) 622.
- [11] N. Chatiras, P. Georgopoulos, A. Christopoulos, E. Kontou, Thermomechanical characterization of basalt fiber reinforced biodegradable polymers, *Polym. Compos.* 40 (2019) 4340–4350.
- [12] L.C. Mohr, A.P. Capelezzo, C.R.D.M. Baretta, M.A.P.M. Martins, M.A. Fiori, J.M.M. Mello, Titanium dioxide nanoparticles applied as ultraviolet radiation blocker in the polylactic acid biodegradable polymer, *Polym. Test.* 77 (2019) 105867.
- [13] J. Jayaramudu, K. Das, M. Sonakshi, G. Siva Mohan Reddy, B. Aderibigbe, R. Sadiku, et al., Structure and properties of highly toughened biodegradable polylactide/ZnO biocomposite films, *Int. J. Biol. Macromol.* 64 (2014) 428–434.
- [14] J. Jiménez Reinosa, P. Leret, C.M. Álvarez-Docio, A. del Campo, J.F. Fernández, Enhancement of UV absorption behavior in ZnO-TiO<sub>2</sub> composites, *Bol. Soc. Esp. Cerám. Vidrio* 55 (2016) 55–62.
- [15] D.R. Sambandan, D. Ratner, Sunscreens: an overview and update, *J. Am. Acad. Dermatol.* 64 (2011) 748–758.
- [16] A. Marra, C. Silvestre, D. Duraccio, S. Cimmino, Polylactic acid/zinc oxide biocomposite films for food packaging application, *Int. J. Biol. Macromol.* 88 (2016) 254–262.
- [17] S. Shankar, L.F. Wang, J.W. Rhim, Incorporation of zinc oxide nanoparticles improved the mechanical, water vapor barrier, UV-light barrier, and antibacterial properties of PLA-based nanocomposite films, *Mater. Sci. Eng. C Mater. Biol. Appl.* 93 (2018) 289–298.
- [18] H. Abe, N. Takahashi, K.J. Kim, M. Mochizuki, Y. Doi, Thermal degradation processes of end-capped poly(l-lactide)s in the presence and absence of residual zinc catalyst, *Biomacromolecules* 5 (2004) 1606–1614.
- [19] M. Murariu, A. Doumbia, L. Bonnau, A.L. Dechief, Y. Paint, M. Ferreira, et al., High-performance polylactide/ZnO nanocomposites designed for films and fibers with special end-use properties, *Biomacromolecules* 12 (2011) 1762–1771.
- [20] E. de Lucas-Gil, P. Leret, M. Monte-Serrano, J.J. Reinoso, E. Enríquez, A. Del Campo, et al., ZnO Nanoporous spheres with broad-spectrum antimicrobial activity by physicochemical interactions, *ACS Appl. Nano Mater.* 1 (2018) 3214–3225.
- [21] N. Lucas, C. Bienaime, C. Belloy, M. Queneudec, F. Silvestre, J.E. Nava-Saucedo, Polymer biodegradation: mechanisms and estimation techniques, *Chemosphere* 73 (2008) 429–442.
- [22] M.P. Arrieta, M.D. Samper, M. Aldas, J. Lopez, On the Use of PLA-PHB blends for sustainable food packaging applications, *Materials* (Basel) (2017) 10.
- [23] UNE-EN ISO 20200:2016 Determination of the degree of disintegration of plastic materials under simulated composting conditions in a laboratory-scale test (ISO 20200:2015).
- [24] E. Lizundia, L. Ruiz-Rubio, J.L. Vilas, L.M. León, Towards the development of eco-friendly disposable polymers: ZnO-initiated thermal and hydrolytic degradation in poly(l-lactide)/ZnO nanocomposites, *RSC Adv.* 6 (2016) 15660–15669.
- [25] S. Benali, S. Aouadi, A.-L. Dechief, M. Murariu, P. Dubois, Key factors for tuning hydrolytic degradation of polylactide/zinc oxide nanocomposites, *Nanocomposites* 1 (2015) 51–61.
- [26] A. Anžlovar, A. Kržan, E. Žagar, Degradation of PLA/ZnO and PHBV/ZnO composites prepared by melt processing, *Arab. J. Chem.* 11 (2018) 343–352.
- [27] E. de Lucas-Gil, J.J. Reinoso, K. Neuhaus, L. Vera-Londono, M. Martín-González, J.F. Fernández, et al., Exploring new mechanisms for effective antimicrobial materials: electric contact-killing based on multiple Schottky barriers, *ACS Appl. Mater. Interfaces* 9 (2017) 26219–26225.
- [28] E. de Lucas-Gil, A. Del Campo, L. Pascual, M. Monte-Serrano, J. Menéndez, J.F. Fernández, et al., The fight against multidrug-resistant organisms: the role of ZnO crystalline defects, *Mater. Sci. Eng. C* 99 (2019) 575–581.
- [29] R.Y. Tabasi, A. Ajji, Selective degradation of biodegradable blends in simulated laboratory composting, *Polym. Degrad. Stab.* 120 (2015) 435–442.
- [30] M.P. Arrieta, J. López, E. Rayón, A. Jiménez, Disintegrability under composting conditions of plasticized PLA-PHB blends, *Polym. Degrad. Stab.* 108 (2014) 307–318.
- [31] M. Yasuniwa, S. Tsubakihara, K. Ohoshita, S.I. Tokudome, X-ray studies on the double melting behavior of poly(butylene terephthalate), *J. Polym. Sci. Part B* 39 (2001) 2005–2015.
- [32] Z. Gan, K. Kuwabara, M. Yamamoto, H. Abe, Y. Doi, Solid-state structures and thermal properties of aliphatic-aromatic poly(butylene adipate-co-butylene terephthalate) copolymers, *Polym. Degrad. Stab.* 83 (2004) 289–300.
- [33] E. Quero, A.J. Müller, F. Signori, M.-B. Coltell, S. Bronco, Isothermal cold-crystallization of PLA/PBAT blends with and without the addition of acetyl tributyl citrate, *Macromol. Chem. Phys.* 213 (2012) 36–48.
- [34] P.M. Ma, R.Y. Wang, S.F. Wang, Y. Zhang, Y.X. Zhang, D. Hristova, Effects of fumed silica on the crystallization behavior and thermal properties of poly(hydroxybutyrate-co-hydroxyvalerate), *J. Appl. Polym. Sci.* 108 (2008) 1770–1777.
- [35] M. Yasuniwa, S. Tsubakihara, Y. Sugimoto, C. Nakafuku, Thermal Analysis of the Double-Melting Behavior of Poly(L-lactic acid), *J. Polym. Sci.: Part B* 42 (2004) 25–32.
- [36] R.C. Nonato, L.H.I. Mei, B.C. Bonse, E.F. Chinaglia, A.R. Morales, Nanocomposites of PLA containing ZnO nanofibers made by solvent cast 3D printing: production and characterization, *Eur. Polym. J.* 114 (2019) 271–278.
- [37] E. Lizundia, P. Mateos, J.L. Vilas, Tunable hydrolytic degradation of poly(l-lactide) scaffolds triggered by ZnO nanoparticles, *Mater. Sci. Eng. C Mater. Biol. Appl.* 75 (2017) 714–720.
- [38] M. Qu, H. Tu, M. Amarantao, Y.-Q. Song, S.S. Zhu, Zinc oxide nanoparticles catalyze rapid hydrolysis of poly(lactic acid) at low temperatures, *J. Appl. Polym. Sci.* 131 (2014) n/a-n/a.
- [39] H. Kaur, A. Rathore, S. Raju, A study on ZnO nanoparticles catalyzed ring opening polymerization of L-lactide, *J. Polym. Res.* 21 (2014) 537.
- [40] E. Fortunati, I. Armentano, A. Iannoni, M. Barbale, S. Zocco, M. Scavone, et al., New multifunctional poly(lactide acid) composites: mechanical, antibacterial, and degradation properties, *J. Appl. Polym. Sci.* 124 (2012) 87–98.
- [41] I. Taiatele, T.C. Dal Bosco, P.C.S. Faria-Tischer, A.P. Bilck, F. Yamashita, J. Bertozzi, et al., Abiotic hydrolysis and compostability of blends based on cassava starch and biodegradable polymers, *J. Polym. Environ.* 27 (2019) 2577–2587.
- [42] A. Carbonell-Verdu, J.M. Ferri, F. Dominicí, T. Boronat, L. Sanchez-Nacher, R. Balart, et al., Manufacturing and compatibilization of PLA/PBAT binary blends by cottonseed oil-based derivatives, *Express. Polym. Lett.* 12 (2018) 808–823.
- [43] N.-Q. Puay, G. Qiu, Y.-P. Ting, Effect of Zinc oxide nanoparticles on biological wastewater treatment in a sequencing batch reactor, *J. Clean. Prod.* 88 (2015) 139–145.

- [44] G.V. Lowry, K.B. Gregory, S.C. Apte, J.R. Lead, Transformations of nanomaterials in the environment, *Environ. Sci. Technol.* 46 (2012) 6893–6899.
- [45] J.S. Chang, M.N. Chong, P.E. Poh, J.D. Ocon, M.Z.H. Md Zorrott, S.M. Lee, Impacts of morphological-controlled ZnO nanoarchitectures on aerobic microbial communities during real wastewater treatment in an aerobic-photocatalytic system, *Environ. Pollut.* 259 (2019) 113867.
- [46] X. Dai, Y. Cao, X. Shi, X. Wang, Non-isothermal crystallization kinetics, thermal degradation behavior and mechanical properties of poly(lactic acid)/MOF composites prepared by melt-blending methods, *RSC Adv.* 6 (2016) 71461–71471.
- [47] Y. Luo, Z. Lin, G. Guo, Biodegradation assessment of poly (lactic acid) filled with functionalized titania nanoparticles (PLA/TiO<sub>2</sub>) under compost conditions, *Nanoscale Res. Lett.* 14 (2019) 56.
- [48] G. Kale, R. Auras, S.P. Singh, Comparison of the degradability of poly (lactide) packages in composting and ambient exposure conditions, *Packag. Technol. Sci.* 20 (2007) 49–70.
- [49] S. Therias, J.F. Larche, P.O. Bussiere, J.L. Gardette, M. Murariu, P. Dubois, Photochemical behavior of polylactide/ZnO nanocomposite films, *Biomacromolecules* 13 (2012) 3283–3291.